Biocomposites from Polylactic Acid and Bacterial Cellulose Nanofibers Obtained by Mechanical Treatment

Denis Mihaela Panaitescu,[a,]* Adriana Nicoleta Frone,[a] Ioana Chiulan,[a] Raluca Augusta Gabor,[a] Ilie Catalin Spataru,[a] and Angela Căşărică [b]

Bacterial cellulose nanofibers (BCNF), obtained by the mechanical disintegration of BC pellicles, were used without any surface treatment for the fabrication of poly(lactic acid) (PLA) nanocomposites by a melt compounding process. The addition of BCNF in different amounts improved both the Young's modulus and tensile strength of PLA. A 22% increase in these properties was observed in the nanocomposite with 2 wt.% nanofibers, due to the BCNF network formed at this concentration and characterized by atomic force microscopy. BCNF addition also increased the crystallinity and thermal stability of PLA, which were evaluated by thermal analysis. Due to the high purity of BCNF and the environmental friendliness of melt processing, it was concluded that PLA/BCNF nanocomposites can be designed for biomedical field and food packaging.

*Contact information: a: Polymer Department, National Institute for Research and Development in Chemistry and Petrochemistry, 060021 Bucharest, Romania; b: National Institute for Chemical - Pharmaceutical R&D, 031299 Bucharest, Romania *Corresponding author: panaitescu@icf.ro*

INTRODUCTION

New "green" materials have been developed from renewable resources to replace petroleum based materials and to protect the environment. Poly(lactic acid) (PLA), an aliphatic polyester, is produced from maize, wheat, sugar beets, or agricultural waste, and it is one of the most studied materials due to its outstanding properties (Inkinen *et al.* 2011; Panaitescu *et al.* 2016a). The large application of PLA in food packaging and biomedicine is hindered by its brittleness and slow crystallization, as well as poor barrier properties (Frone *et al.* 2016). Cellulose micro- and nano-reinforcements have been extensively studied to improve PLA properties (Tawakkal *et al.* 2012; Frone *et al.* 2013; Indarti *et al.* 2016). Bacterial cellulose (BC) is a promising reinforcing material in aliphatic polyesters for biomedical and packaging applications (Chiulan *et al.* 2016; Panaitescu *et al.* 2016b). PLA/BC laminated composites have been prepared by sinking the dried BC pellicles in a PLA solution in chloroform (Kim *et al.* 2009) or by compression molding BC strips between two PLA films (Quero *et al.* 2010). Wider processing possibilities and improved mechanical properties may be obtained by dispersing individual BC nanofibers (BCNF) in PLA. The fine dispersion of BCNF in PLA and other hydrophobic polymers is difficult due to the strong bonds between nanofibers in the BC pellicle and their hydrophilic character, opposite to the hydrophobicity of the matrix (Panaitescu *et al.* 2016b).

Only a few attempts to disperse BCNF or BC nanowhiskers (BCNW) in PLA have been reported (Lee *et al*. 2009; Blaker *et al*. 2010; Martínez-Sanz *et al*. 2012; Luo *et al*. 2014). BCNW, prepared by acid hydrolysis, were incorporated in PLA by electrospinning, which resulted in masterbatches (Martínez-Sanz *et al*. 2012). Nanocomposites, obtained by melt-mixing these masterbatches with PLA, showed up as a 17% increase in Young's modulus and up to 14% increase in tensile strength in PLA/3% BCNW (Martínez-Sanz *et al*. 2012). After solvent exchange, BCNW were dispersed in chloroform or dimethyl carbonate to obtain porous PLA nanocomposites (Blaker *et al*. 2010). Likewise, BCNF prepared by wet mechanical disintegration were surface functionalized and mixed with PLA in 1,4-dioxane (Lee *et al*. 2009). A temperature induced phase separation technique was further used to prepare composite microspheres, which allowed processing of PLA/BC composites using a conventional extrusion process (Lee *et al*. 2009). A 50% increase of tensile modulus was reported in this case.

BCNF were obtained in a previous work by mechanical disintegration, using two approaches (Panaitescu *et al*. 2016b). BCNF prepared by wet disintegration, followed by freeze drying and dry mechanical treatment (Panaitescu *et al*. 2016b), were incorporated in different amounts in PLA using a melt processing technique. The effect of different amounts of BCNF on the morphology, thermal, and mechanical properties of PLA nanocomposites was studied in this paper. PLA/BCNF nanocomposites have been designed for both the biomedical field and food packaging. Compared to other micro- or nano-celluloses, BCNF have high purity due to their precursor (BC) and a chemicals-free preparation route.

EXPERIMENTAL

Materials

PLA 4032D with high molecular mass (195,000 to 205,000 Da) and a density of 1.24 g/cm^3 was purchased from Nature Works, LLC (Minnetonka, MN, USA). BCNF were prepared from fresh bacterial cellulose pellicles by mechanical disintegration, as described elsewhere (Panaitescu *et al*. 2016b, method I). After the mechanical treatment, the nanofibers were released from the initial BC pellicle (Fig. 1a) as individual nanofibers of micrometric length and less than 150 nm in width and as tapes (Fig. 1b).

Preparation of Nanocomposites

PLA pellets and BCNF were dried in a vacuum oven for 4 h at 80 °C and 24 h at 40 °C, respectively. Dried BCNF were added into melted PLA using a mixing chamber of 50 cm^3, connected to a Brabender LabStation (Duisburg, Germany). Melt mixing was performed at 170 °C for 7 min and a rotor speed of 100 rpm. The compounded mixtures containing 0, 0.5, 2, and 5 wt.% BCNF were shaped in foils on a laboratory two-roll mill (Polymix 110L, Duisburg, Germany) at 140 °C with 27/22.5 rpm. Sheets with the thickness of 0.5 mm were obtained by compression molding using an electrically heated press (P200E Dr. Collin, Munich, Germany) at 180 °C, with 3 min of preheating (5 bar), 2 min under pressure (150 bar), and cooling for another 1.5 min in a cooling cassette. A neat PLA sheet prepared in the same conditions served as a reference.
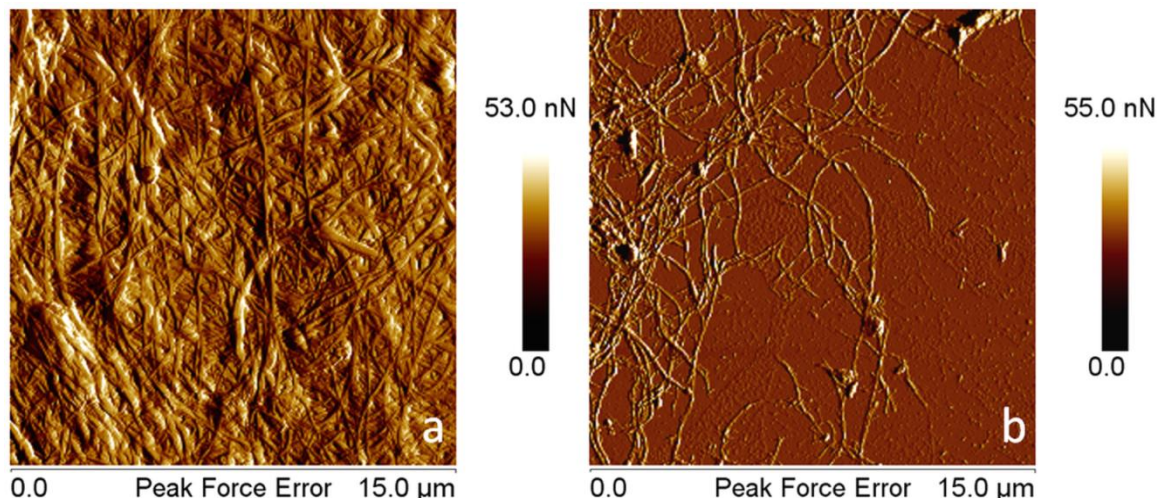
Fig. 1. AFM - Peak force error images of BC pellicle (a) and BCNF (b)

Characterization of PLA/BCNF Nanocomposites

The surface morphology of PLA nanocomposites was investigated by atomic force microscopy (AFM), Quantitative Nanomechanical Mapping – Peak Force QNM mode, using a Bruker MultiMode 8 instrument (Santa Barbara, CA, USA). A silicon tip with the spring constant of 40 N/m and a resonant frequency of 300 kHz was used at a scanning rate of about 0.7 Hz.

Tensile properties of nanocomposites were measured at room temperature with a crosshead speed of 2 mm/min, using an Instron 3382 universal testing machine (Norwood, MA, USA) with a video extensometer. Five specimens 5A according ISO 527 (2012) were tested for each sample.

The thermo-mechanical properties of PLA matrix and nanocomposites were analyzed using a dynamic mechanical analyzer DMA Q800 (TA Instruments, New Castle, DE, USA) operating in the tensile mode, at a heating rate of 3 °C /min. The experiments were performed on parallel specimens with length $\times$ width $\times$ thickness of 18 mm $\times$ 4 mm $\times$ 0.5 mm, from the room temperature to 100 °C. The effectiveness of the filler in nanocomposites (*Coefficient C*) was determined from the storage modulus in the glassy (E_G) and rubbery (E_R) regions (Etaati *et al*. 2014), as shown in Eq. 1.

$$Coefficient\ C = \frac{(E_G / E_R)_{nanocomposite}}{(E_G / E_R)_{PLA}}$$

(1)

Thermo-gravimetric analysis (TGA) was performed on a TA-Q5000 V3.13 (TA Instruments Inc., New Castle, DE, USA) device using nitrogen as the purge gas at a flow rate of 40 mL/min. The thermograms were acquired between 25 °C and 700 °C at a heating rate of 10 °C/min. Differential scanning calorimetry (DSC) analysis was carried out on an SDT Q600 V20.9 (TA Instruments) under helium flow (100 mL/min). Samples weighing around 10 mg were packed in aluminum pans and tested from the ambient temperature to 300 °C at a heating rate of 10 °C/min. The degree of crystallinity (X_c) was obtained as follows,

$$X_c \, [\%] = \frac{\Delta H}{w * \Delta H_0} * 100$$

(2)

where ΔH and ΔH_o are the heats of fusion for the nanocomposite and for 100% crystalline PLA, respectively. ΔH_o was set at 93 J/g (Frone *et al*. 2013), and *w* was the mass fraction of PLA in the composite.

RESULTS AND DISCUSSION

Thermal and Thermo-Mechanical Behavior of PLA/BCNF

Because bacterial cellulose begins to degrade at a lower temperature (290 °C) than PLA (350 °C) (Panaitescu *et al*. 2016b), TGA was performed to investigate the influence of different concentrations of BCNF on the thermal stability of nanocomposites. Figure 2a shows that the thermal stability of PLA nanocomposites was not reduced by BCNF, regardless of its concentration. The temperature of maximum degradation rate (T_d) and at 5% weight loss ($T_{5\%}$) are shown in Table 1. The nanocomposite with 0.5 wt.% BCNF exhibited a T_{on} and $T_{5\%}$ that were increased by 2 °C and 5 °C, respectively, compared with pure PLA. Higher concentrations of BCNF also improved the thermal stability of PLA, but to a lesser extent. This behavior can be related to a fine dispersion of BCNF in the PLA and to the higher crystallinity of the fibers compared with that of the matrix. Thus, BCNF may form a protective barrier, lowering the diffusion of volatile degradation products and increasing the thermal stability. This behavior is opposite of that observed in PLA reinforced with 2 wt.% BCNW, prepared by acid hydrolysis, where the T_{on} of the composite was decreased by about 9 °C (Martínez-Sanz et al. 2012).
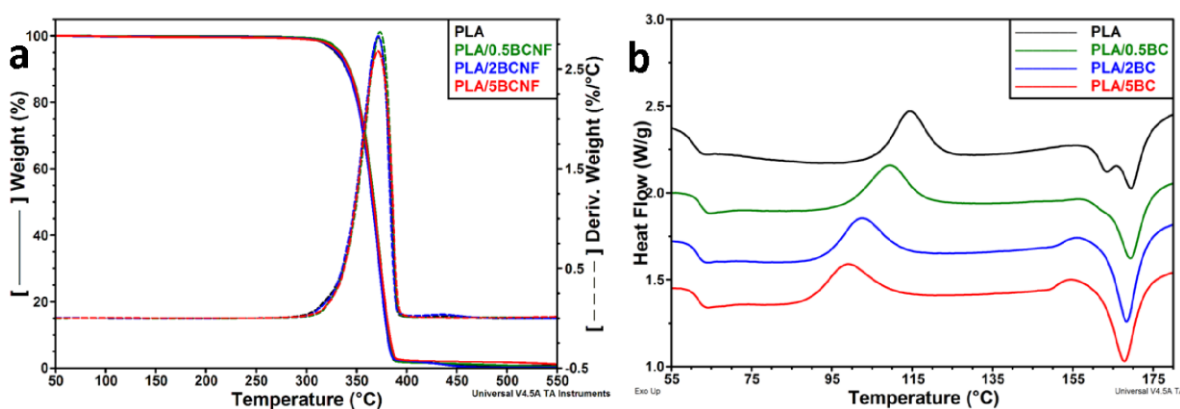
Fig. 2. TGA/DTG curves of PLA/BCNF nanocomposites (a) and DSC thermograms (b)

Table 1. TGA Results for PLA/BCNF Nanocomposites

Sample	T_{on} (°C)	$T_{5\%}$ (°C)	T_d (°C)
PLA	347.3	329.0	371.8
PLA/0.5BCNF	349.0	334.2	373.5
PLA/2BCNF	347.2	330.5	371.6
PLA/5BCNF	348.1	332.7	371.2

DSC thermograms from Fig. 2b show that BCNF influenced the thermal behavior of PLA. The values of the glass transition (T_g), cold crystallization temperature (T_{cc}), melting temperature (T_m), and the corresponding enthalpies are shown in Table 2.

A slight increase of T_g and a noticeable decrease of T_{cc} values were observed when the concentration of BCNF was increased (Table 2). Higher T_g values in polymer nanocomposites are, generally, related to the reduced mobility of macromolecular chains due to the nanofiller/matrix interface adhesion (Frone *et al*. 2016). Lower T_{cc} values of more than 15 °C in PLA/5 wt.% BCNF indicated the accelerated crystallization of PLA, which was due to the nucleating activity of BCNF. The influence of the nanofillers or nanodomains size on the nucleating efficiency in PLA nanocomposites or blends has been extensively studied; smaller nano-particles or nano-domains have higher nucleating efficiency (Ni *et al*. 2009; Ortenzi *et al*. 2015). Thus, the decrease of T_{cc} in nanocomposites (Fig. 2b) can be related to both the high efficiency of BCNF as nucleating agent and to the fine dispersion of BCNF in PLA. Moreover, the decrease of T_{cc} with the increase of BCNF amount in the composites was steeper, almost linear, between 0 and 2 wt.% BCNF and tended to flatten between 2 and 5 wt.% BCNF, suggesting lower interfacial area and the possible agglomeration of fibers.

Table 2. DSC Results for PLA/BCNF Nanocomposites

Sample	T_g (°C)	T_{cc} (°C)	ΔH_{cc}^{*} (J/g)	T_m (°C)	ΔH_m (J/g)	X_c (%)
PLA	61.8	114.4	16.5	163.7/169.6	22.2	23.9
PLA/0.5BCNF	63.6	109.3	17.3	169.4	20.3	22.0
PLA/2BCNF	62.9	102.4	16.9	168.4	25.4	27.9
PLA/5BCNF	63.2	98.9	16.4	168.0	25.9	29.3

* ΔH_{cc}, Cold crystallization enthalpy

A double endothermic peak was observed for the PLA matrix, at 163.3 °C (T_{m1}) and 169.6 °C (T_{m2}). Two melting peaks were previously reported for PLA and explained by polymorphism and melt recrystallization of the unstable crystals formed during the cold-crystallization process (Frone *et al*. 2016). Regardless of BCNF concentration, PLA nanocomposites showed only one melting peak (T_m) close to the higher melting peak of the matrix and similar crystallinity percentage due to cold crystallization (about 18.6 %). These results suggest that BCNF favored the formation of larger crystals with a higher melting temperature. This claim is also supported by the small exothermic hump, observed before the melting peak of the nanocomposites with 2 and 5 wt.% BCNF (Fig. 2b), which indicates additional recrystallization of thinner or less perfect crystals. A similar exothermic hump was observed in PLA composites with cellulose nanofibers from plants (Frone *et al*. 2013). The increase of PLA crystallinity because of BCNF addition is important in nanocomposites with 2 and 5 wt.% BCNF (with 24% and 30%, respectively), also showing the nucleating activity of BCNF.

Dynamic mechanical analysis (DMA) elucidated the influence of BCNF concentration on the viscoelastic properties of PLA matrix. The variation of storage (E') and loss (E'') moduli with temperature is shown in Fig. 3. The influence of temperature on the stiffness of nanocomposites was low in the glassy region, but a sharp decrease of E' values was noted between 50 and 70 ºC, which corresponds to the α relaxation of the amorphous PLA. The addition of 2 and 5 wt.% BCNF in PLA led to an increase of E' modulus before T_g. Moreover, the peak of loss modulus was shifted to higher

temperature, regardless of nanofiber concentration (Table 3). Similar T_g values around 63.3 ºC were obtained for all nanocomposites, which was 2 ºC higher than that of the matrix. This data confirmed the DSC results (Fig. 2b, Table 2).
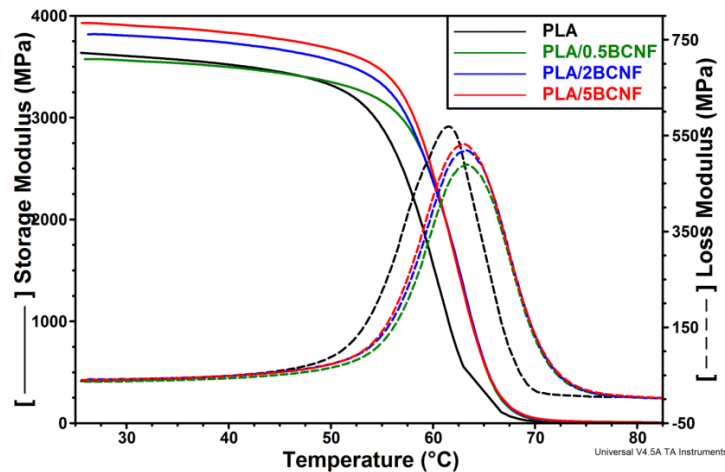
Fig. 3. DMA results: storage modulus (—) and loss modulus (- -) of PLA nanocomposites

Both the increase of E' and the shift of the E'' peak show the influence of BCNF in restricting the segmental motion of the PLA chains and increasing the stiffness. These effects are directly related to the adhesion at the fiber-matrix interface. Because no treatment was applied to BCNF, it can be assumed that the dispersion of nanofibers in PLA was good, providing high interfacial area. Moreover, lower E'' values (corresponding to the peak) were noted for nanocomposites compared with the matrix (Fig. 3), showing lower energy dissipation. These results suggest lower interfacial friction and, therefore, good PLA/BCNF interface (Etaati *et al.* 2014).

Table 3. DMA Results for PLA/BCNF Nanocomposites

Sample	T_g (°C)	E'_{40} (MPa)	E'_{70} (MPa)	Coefficient C
PLA	61.5	3521	22	-
PLA/0.5BCNF	63.4	3496	39	0.56
PLA/2BCNF	63.3	3734	44	0.53
PLA/5BCNF	63.2	3834	51	0.47

The effectiveness of BCNF in the composite was measured by the *coefficient C* (Table 3), which characterizes the drop in modulus in the glass transition region. High values of *coefficient C* means low effectiveness of the filler (Etaati *et al.* 2014). Slightly lower *C* values were obtained with the increase of BCNF concentration in the composites. PLA/5 wt.% BCNF showed the smallest difference between E' values in the glassy and in the rubbery state and the lowest C value (the highest effectiveness).

Tensile Properties

The mechanical properties of nanocomposites are shown in Table 4. The tensile strength of PLA increased by 15% and the Young's modulus (*YM*) increased by 10% when BCNF were added in very low amount (0.5 wt.%). No significant change in elongation at break was observed at this concentration of nanofibers. The composite with

bioresources.com

2 wt.% BCNF showed an increase in both strength and modulus of about 22 to 23%, while the elongation at break was halved. Similar results were reported for PLA/2wt.% BCNW, prepared by masterbatch and electrospinning; these techniques ensured a homogenous dispersion of BCNW in PLA (Martínez-Sanz *et al*. 2012). Therefore, PLA/2 wt.% BCNF was also characterized by a good dispersion of nanofibers. The tensile tests results emphasized both the reinforcing effect of BCNF and their dispersion in the matrix, knowing that nanofillers can act as reinforcements to strengthen the polymer matrix only if they are dispersed homogeneously on the nanoscale.

Table 4. Mechanical Properties of PLA/BCNF Nanocomposites

Sample	Elongation at Break (%)	Tensile Strength (MPa)	Young's Modulus (MPa)
PLA	7.6 ± 0.9	46.6 ± 1.7	2892 ± 96
PLA/0.5BCNF	6.5 ± 0.5	53.7 ± 1.4	3192 ± 102
PLA/2BCNF	4.2 ± 0.4	57.5 ± 2.1	3512 ± 87
PLA/5BCNF	2.1 ± 0.2	55.3 ± 2.8	3678 ± 110

Further addition of BCNF increased the modulus but drastically decreased the elongation (Table 4). The dependence of *YM* on BCNF volume fraction (*f*) is complex because the experimental data could be fitted with a second-order polynomial function.
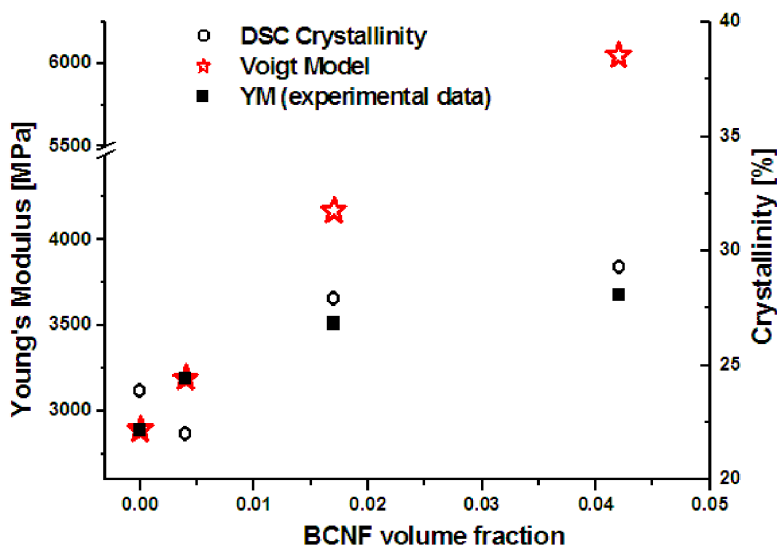
Fig. 4. The dependence of YM on BCNF volume fraction: experimental results and Voigt model; correlation with DSC crystallinity

The Young's modulus of the composites was also calculated using the rule of mixtures (Voigt model – upper-bound modulus),

$$YM = f \times M_f + (1 - f) \times M_m \tag{3}$$

where M_f and M_m are the Young's moduli of the fibers and of the matrix. The modulus of BCNF was considered to be 78 GPa, in accordance to the value reported for single bacterial cellulose fibers (Guhados *et al*. 2005). The *YM* value was well estimated by the Voigt model only for the composite with 0.05 wt.% BCNF (Fig. 4); for higher

concentrations of nanofibers, the differences between the theoretical and experimental values were large. The reinforcement effectiveness of BCNF was estimated by calculating an effective modulus of the fibers (M_f*) using the experimental *YM* data in Eq. 3. Smaller M_f* values were obtained for the composites with 2 and 5 wt.% BCNF (40 GPa and 22 GPa, respectively, instead of 78 GPa), showing that the reinforcing capacity of BCNF had not been completely used. Various factors might contribute to this behavior, *e.g.*, the air incorporated with the nanofibers during melt processing, lack of compatibilization between the fibers and the matrix, and the lower increase of crystallinity in the composites with higher amount of fibers (Fig. 4). Some agglomeration of nanofibers is also possible because no treatment or coupling agent was used.

Nanocomposites were investigated by AFM to observe the dispersion of the fibers and their size (Figs. 5 and 6). Both individual nanofibers and bundles were observed on the surface of PLA/0.5 wt.% BCNF (Fig. 5, c and d images). The length of the fibers varied within wide limits, from 120 nm to more than 500 nm and their width from 35 nm to 50 nm, as highlighted by AFM software. A homogeneous dispersion of nanofibers was observed in the nanocomposite with 2 wt.% BCNF (Fig. 5). A network was noted at this concentration of nanofibers. Analysis of the images with NanoScope software (Bruker, Santa Barbara, CA, USA) emphasized the average width of BCNF in this composite (47 ± 4 nm) and their length in the range from 130 to 400 nm.
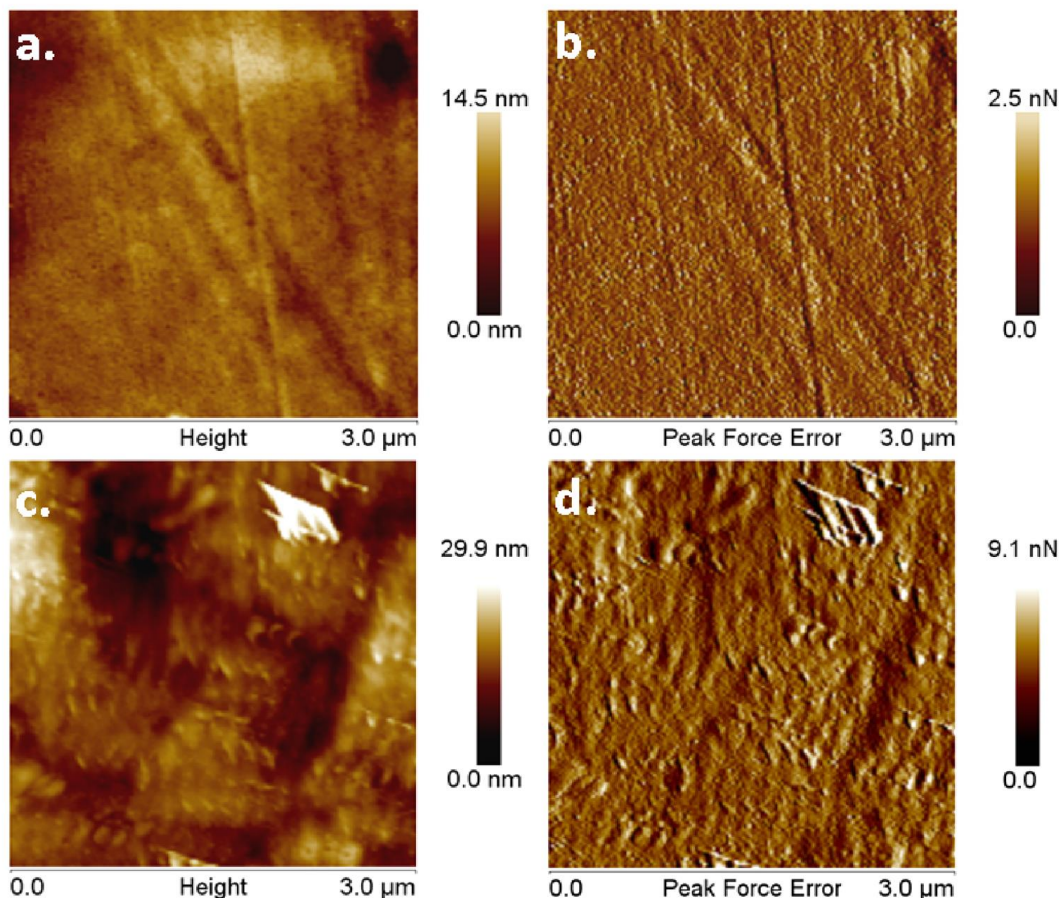
Fig. 5. AFM topographic and peak force error images of PLA (a and b) and PLA/0.5 wt.% BCNF (c and d)
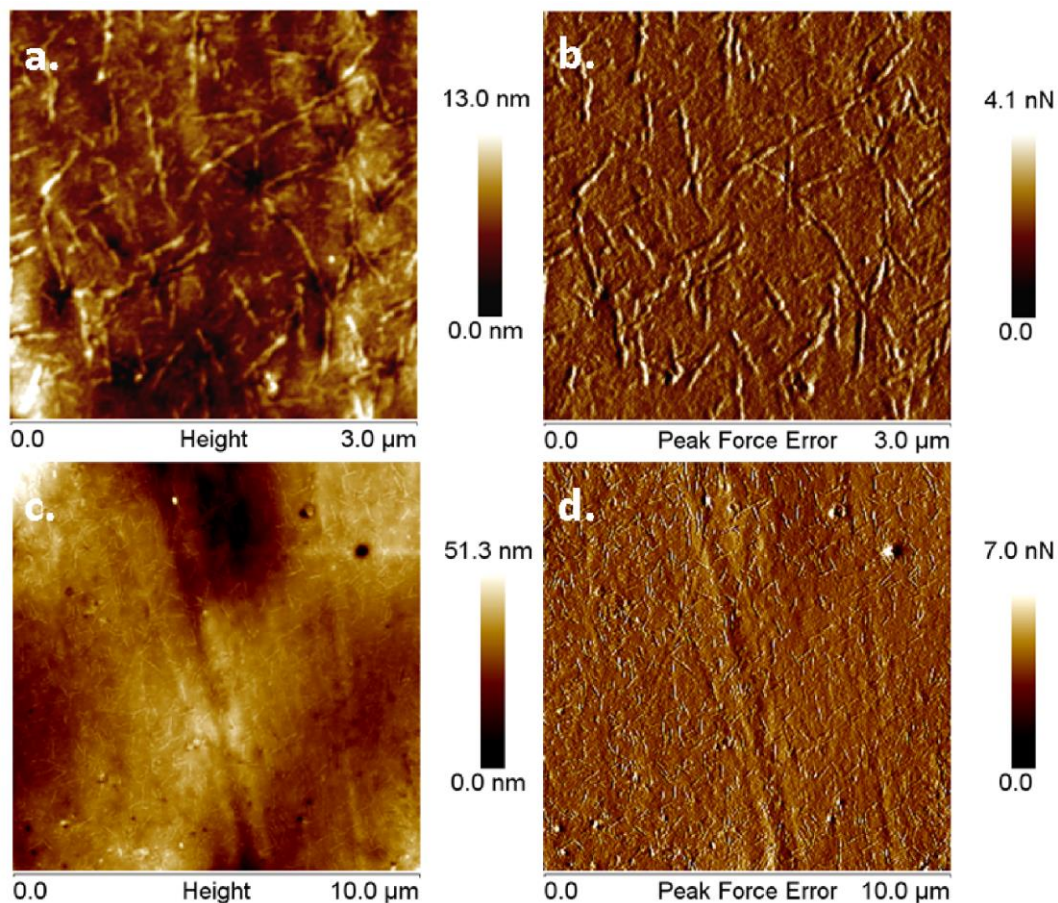
Fig. 6. Topographic and peak force error images (different magnification) of PLA/2 wt.% BCNF

Topographic and peak force error images captured on the surface of the composite with 5 wt.% BCNF showed mostly small fibers, with the length from 150 nm to 250 nm, homogenously dispersed in PLA ((Panaitescu *et al*. 2016b).

Both the length and the width of the nanofibers in the composites (Fig. 5 and 6) were smaller than before the melt processing step (Fig. 1). This result showed the effect of the shear forces in splitting and breaking the fibers, thus ensuring a good dispersion of BCNF in the matrix. The best dispersion was noticed for PLA/2 wt.% BCNF, and it can be hypothesized that a concentration of about 2 to 3% BCNF is optimum in PLA due to the good mechanical properties and dispersion.

CONCLUSIONS

1. BCNF obtained by mechanical defibrillation of BC pellicles is a valuable reinforcement in PLA, improving its modulus, increasing the crystallinity, and thermal stability.

2. BCNF formed a network from a concentration of only 2 wt.% in PLA, which improved the mechanical properties in the absence of a compatibilizer or surface treatment.

bioresources.com

3. BCNF accelerated the crystallization of PLA, leading to increased crystallinity, and a decrease in the cold crystallization temperature.

4. PLA/BCNF nanocomposites are valuable materials for both biomedical field and food packaging, considering the high purity of BCNF and the environmental friendliness of the melt processing process.

ACKNOWLEDGMENTS

REFERENCES CITED

Blaker, J. J., Lee, K.-Y., Mantalaris, A., and Bismarck, A. (2010). "Ice-microsphere templating to produce highly porous nanocomposite PLA matrix scaffolds with pores selectively lined by bacterial cellulose nano-whiskers," *Composites Science and Technology* 70(13), 1879-1888. DOI: 10.1016/j.compscitech.2010.05.028

Chiulan, I., Panaitescu, D. M., Frone, A. N., Teodorescu, M., Nicolae, C. A., Căşărică, A., Tofan, V., and Sălăgeanu, A. (2016). "Biocompatible polyhydroxyalkanoates/ bacterial cellulose composites: Preparation, characterization, and *in vitro* evaluation," *Journal of Biomedical Materials Research A* 104(10), 2576-2584. DOI: 10.1002/jbm.a.35800

Etaati, A., Pather, S., Fang, Z., and Wang, H. (2014). "The study of fibre/matrix bond strength in short hemp polypropylene composites from dynamic mechanical analysis," *Composites: Part B* 62, 19-28. DOI: 10.1016/j.compositesb.2014.02.011

Frone, A. N., Panaitescu D. M., Chiulan I., Nicolae C. A., Vuluga Z., Vitelaru C., and Damian, C. M. (2016). "The effect of cellulose nanofibers on the crystallinity and nanostructure of poly(lactic acid) composites," *Journal of Materials Science* 51(21), 9771-979. DOI: 10.1007/s10853-016-0212-1

Frone, A. N., Berlioz S., Chailan J-F., and Panaitescu, D. M. (2013). "Morphology and thermal properties of PLA–cellulose nanofibers composites," *Carbohydrate Polymers* 91(1), 377-384. DOI: 10.1016/j.carbpol.2012.08.054

Guhados, G., Wan W., and Hutter, J. L. (2005). "Measurement of the elastic modulus of single bacterial cellulose fibers using atomic force microscopy," *Langmuir* 21(14), 6642-6646. DOI: 10.1021/la0504311

Indarti, E., Rohaizu, R., Marwan, and Wan Daud, W. R. (2016). "Polylactic acid bionanocomposites filled with nanocrystalline cellulose from TEMPO-oxidized oil palm lignocellulosic biomass," *BioResources* 11(4), 8615-8626.

Inkinen, S., Hakkarainen, M., Albertsson, A-C., and Södergard, A. (2011). "From lactic acid to poly(lactic acid) (PLA): Characterization and analysis of PLA and its precursors," *Biomacromolecules* 12(3), 523-532. DOI: 10.1021/bm101302t

ISO 527 (2012). "Plastics - Determination of tensile properties - Part 2: Test conditions for moulding and extrusion plastics," International Organization for Standardization, Geneva, Switzerland.

Kim, Y., Jung, R., Kim, H. S., and Jin, H. J. (2009). "Transparent nanocomposites prepared by incorporating microbial nanofibrils into poly(L-lactic acid)," *Current Applied Physics* 9, S69-S71. DOI: 10.1016/j.cap.2008.08.010

Lee, K.-Y., Blaker, J. J., and Bismarck, A. (2009). "Surface functionalisation of bacterial cellulose as the route to produce green polylactide nanocomposites with improved properties," *Composites Science and Technology* 69(15-16), 2724-2733. DOI: 10.1016/j.compscitech.2009.08.016

Luo, H., Xiong, G., Li, Q., Ma, C., Zhu, Y., Guo, R., and Wan, Y. (2014). "Preparation and properties of a novel porous poly(lactic acid) composite reinforced with bacterial cellulose nanowhiskers," *Fibers and Polymers* 15(12), 2591-2596. DOI: 10.1007/s12221-014-2591-8

Martínez-Sanz, M., Lopez-Rubio, A., and Lagaron, J. M. (2012). "Optimization of the dispersion of unmodified bacterial cellulose nanowhiskers into polylactide *via* melt compounding to significantly enhance barrier and mechanical properties," *Biomacromolecules* 13(11), 3887-3899. DOI: 10.1021/bm301430j

Ni, C., Luo, R., Xu, K., and Chen, G.-Q. (2009). "Thermal and crystallinity property studies of poly (l-lactic acid) blended with oligomers of 3-hydroxybutyrate or dendrimers of hydroxyalkanoic acids," *Journal of Applied Polymer Science* 111(4), 1720-1727. DOI: 10.1002/app.29182

Ortenzi, M. A., Basilissi, L., Farina, H., Di Silvestro, G., Piergiovanni, L., and Mascheroni, E. (2015). "Evaluation of crystallinity and gas barrier properties of films obtained from PLA nanocomposites synthesized *via in situ* polymerization of L-lactide with silane-modified nanosilica and montmorillonite," *European Polymer Journal*, 66, 478-491. DOI: 10.1016/j.eurpolymj.2015.03.006

Panaitescu, D. M., Frone, A. N., and Chiulan, I. (2016a). "Nanostructured biocomposites from aliphatic polyesters and bacterial cellulose," *Industrial Crops and Products* 93, 251-266. DOI: 10.1016/j.indcrop.2016.02.038

Panaitescu, D. M., Frone, A. N., Chiulan, I., Casarica, A., Nicolae, C. A., Ghiurea, M., Trusca, R., and Damian, C. M. (2016b). "Structural and morphological characterization of bacterial cellulose nano-reinforcements prepared by mechanical route," *Materials and Design* 110, 790-801. DOI: 10.1016/j.matdes.2016.08.052

Quero, F., Nogi, M., Yano, H., Abdulsalami, K., Holmes, S. M., Sakakini B. H., and Eichhorn, S. J. (2010). "Optimization of the mechanical performance of bacterial cellulose/poly(l-lactic) acid composites," *ACS Applied Materials & Interfaces* 2(1), 321-330. DOI: 10.1021/am900817f

Tawakkal, I. S. M. A., Talib, R. A., Abdan, K., and Ling, C. N. (2012). "Mechanical and physical properties of kenaf-derived cellulose (KDC)-filled polylactic acid (PLA) composites," *BioResources* 7(2), 1643-1655.